Investigation of deformation effects on the decay properties of 12C+α Cluster states in 16O

Soylu, A.; Koyuncu, F.; Coban, A.; Bayrak, O.; Freer, M.

DOI:
10.1016/j.aop.2018.02.011

Document Version
Peer reviewed version

Citation for published version (Harvard):
Soylu, A, Koyuncu, F, Coban, A, Bayrak, O & Freer, M 2018, 'Investigation of deformation effects on the decay properties of ^{12}C+α Cluster states in ^{16}O', *Annals of Physics*, vol. 391, pp. 263-277. https://doi.org/10.1016/j.aop.2018.02.011

Accepted Manuscript

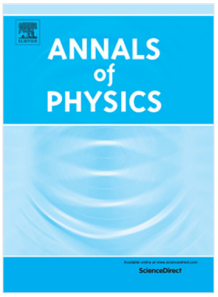

Investigation of deformation effects on the decay properties of $^{12}C + \alpha$ Cluster states in ^{16}O

A. Soylu, F. Koyuncu, A. Coban, O. Bayrak, M. Freer

PII: S0003-4916(18)30036-8
DOI: https://doi.org/10.1016/j.aop.2018.02.011
Reference: YAPHY 67598

To appear in: *Annals of Physics*

Received date : 22 September 2017
Accepted date : 14 February 2018

Please cite this article as: A. Soylu, F. Koyuncu, A. Coban, O. Bayrak, M. Freer, Investigation of deformation effects on the decay properties of $^{12}C + \alpha$ Cluster states in ^{16}O, *Annals of Physics* (2018), https://doi.org/10.1016/j.aop.2018.02.011

Investigation of Deformation Effects on the Decay Properties of ^{12}C+α Cluster states in ^{16}O

A. Soylu* and F. Koyuncu

Department of Physics, Nigde Ömer Halisdemir University, 51240, Nigde, Turkey

A. Coban and O. Bayrak

Department of Physics, Akdeniz University, 07058, Antalya, Turkey

M. Freer

School of Physics and Astronomy, University of Birmingham, Birmingham, B15 2TT, UK

(Dated: January 25, 2018)

Abstract

We have analyzed the elastic scattering angular distributions data of the α+^{12}C reaction over a wide energy range (E_{lab}=28.2 to 35.5 MeV) within the framework of the Optical Model formalism. A double folding (DF) type real potential was used with a phenomenological Woods-Saxon-squared (WS2) type imaginary potential. Good agreement between the calculations and experimental data was obtained. By using the real DF potential we have calculated the properties of the α-cluster states in ^{16}O by using the Gamow code as well as the α-decay widths by using the WKB method. We implemented a ^{12}C+α cluster framework for the calculation of the excitation energies and decay widths of ^{16}O as a function of the orientation of the planar ^{12}C nucleus with respect to the α-particle. These calculations showed strong sensitivity of the widths and excitation energies to the orientation. Branching ratios were also calculated and though less sensitive to the ^{12}C orientation, it was found that ^{12}C$_{gs}$+α structure, with the α-particle orbiting the ^{12}C in its ground state, is dominant. This work demonstrates that deformation, and the orientation, of ^{12}C at plays a crucial role in the understanding the nature of the α-cluster states in ^{16}O.

PACS numbers: 21.60.Gx, 23.60.+e

Keywords: elastic scattering, deformation, excitation energies, alpha decay width, alpha cluster model

* Corresponding Author:Tel:+90 388 225 42 20
email:asimsoylu@gmail.com

I. INTRODUCTION

The nucleus is a complicated many-body system which requires the interaction between the many nucleon constituents to be deduced. This is challenging as it includes not only two-body, but also three-body interactions. However, in a certain class of nuclei the nucleons cluster to form sub units and then to first order the interaction is reduced to that between clusters. Such states of nuclear matter greatly simplify the complexity and in turn reveal important detail regarding the nature of the nuclear force which precipitates the clusters. In a simplifying approach such nuclei may then be explained in terms of a clustering model.

In its simplest form the cluster model describes the nucleus as a binary cluster in which the cluster, composed of a few nucleons, orbits a core containing the remaining nucleons [1, 2]. In this way, the problem is reduced to two-body problem. This sort of the model has been used by several authors to describe the structure of light nuclei [3–6] and applied to heavier nuclei is proposed by the observed α and exotic cluster decays of these nuclei [7]. Moreover, in α-cluster studies, a unified description of nuclear structure and scattering has been useful since the nuclear interaction potential can be determined from elastic scattering data. In the literature, a unified study of structure and scattering of the α+^{16}O and α+^{40}Ca system was used to obtain information about the α-cluster structures in ^{20}Ne and ^{44}Ti, respectively [8–11]. Understanding of the alpha-decay mechanism of the light, heavy and superheavy nuclei is an crucial and important phenomena in terms of the cluster model both theoretically and experimentally [12–21]. The α-decay is considered conventionally in the framework of the Gamow model in which the α-particle is assumed to quantum mechanical tunneling through a Coulomb barrier between the cluster and the daughter nucleus [22]. In this instance, the α-particle exists already in the parent nucleus before the decay and it penetrates the barrier. Hence the formula of α-decay width can be written as the product between the frequency of the potential-wall collisions and the barrier penetrability P which is calculated by using WKB method [22–24]. The semiclassical WKB method is very popular in nuclear physics, for example, fusion of heavy ions, fission theory and alpha decay etc. Furthermore, the half-lives calculations of alpha-decay with and without considering the deformation of the nuclei have been performed [25–42].

There has been renewed interest considering the α-particle structure of light nuclei recently. It is known that both the ground-state of ^{8}Be and the second excited state of ^{12}C

have a well developed α-cluster structure. Progress in identifying similar, highly clustered, states in ^{16}O is less advanced. In particular, the structure of oxygen nuclei above the 4α-decay threshold is still an open problem [43–52]. Numerous studies have been conducted in order to investigate the alpha-cluster structure of ^{16}O [53–61]. Buck *et. al* used a simple cluster model to explain the properties of a number of states in light nuclei including ^{16}O [53]. In the model, such states were considered as bound levels and resonances of a cluster-core system, e.g. $\alpha + {}^{12}$C in the case of ^{16}O. They calculated the energies and widths for the states of two rotational bands in ^{16}O by using the potential that is very similar in shape that which would be obtained from to the double-folding (DF) model [54]. In Ref. [58], the elastic cross sections for $\alpha + {}^{12}$C elastic scattering data in the energy region of $E_{c.m.}$= 21.15 to 26.625 MeV were analyzed with the optical model to investigate the unknown 8^+ and 9^- states for rotational bands of ^{16}O by Katsuma [58]. He determined the total quantum number, N, of the $\alpha + {}^{12}$C rotational bands and showed that the 0^+ state has $N = 8$ [58]. In Ref. [59], the authors analyzed the elastic and inelastic $\alpha + {}^{12}$C scattering, and they obtained the states with the $\alpha + {}^{12}$C cluster structure in a unified way by using the double folding (DF) model in the coupled channel method by considering the excited states of ^{12}C.

In the present study the motivation is to be able to find out the effects of the deformation of ^{12}C on the observable of ^{16}O such as the excitation energies, the decay widths, preformation factors and branching ratios. Therefore, firstly we have analyzed the elastic $\alpha + {}^{12}$C scattering experimental data by using DF potential in the Optical Model. We have used same real DF potential to calculate the resonant energy states in ^{16}O and the alpha-decay widths in the framework of the WKB method and Bohr-Sommerfeld quantization. In order to be able to consider the deformation effects in ^{12}C nucleus, the deformed Woods-Saxon-squared (WS2) potential which its parameters were obtained by fitting with DF potential have been used. We have used the WS2 in order to obtain the alpha-decay widths of ^{16}O for a spherical case, at different angles and over all angles. The same potential was used to obtain resonant energy states with Gamow code [62].

In Sec. II, the theoretical background and formulas for the calculations of the Optical Model and Double Folding potential together with the WKB model is presented. The obtained numerical results are given in Sec. III. In Sec. IV, discussion on study and conclusion on the obtained results are presented in detailed.

II. THEORETICAL APPROACH

A. The Optical Model and Double Folding Potential

In the optical model, the effective potential $V_{eff}(r)$ between the projectile and target nuclei is given by

$$V_{eff}(r) = V_{Nuclear}(r) + V_{Coulomb}(r) + V_{Centrifugal}(r), \tag{1}$$

In Eq. 1, the forms of the Coulomb and centrifugal potentials are well-known. Owing to a charge $Z_P e$ interacting with a charge $Z_T e$ distributed uniformly over a sphere of radius R_c, the Coulomb potential is as follows

$$\begin{aligned} V_{Coulomb}(r) &= \tfrac{1}{4\pi\varepsilon_0}\tfrac{Z_P Z_T e^2}{r}, r \geq R_C \\ &= \tfrac{1}{4\pi\varepsilon_0}\tfrac{Z_P Z_T e^2}{2R_C}(3 - \tfrac{r^2}{R_C^2}), r < R_C, \end{aligned} \tag{2}$$

where R_c is the Coulomb radius, and Z_P and Z_T denote the charges of the projectile P and the target nuclei T, respectively. The final term in Eq. 1 is the centrifugal potential

$$V_{Centrifugal}(r) = \frac{\hbar^2}{2\mu}\frac{l(l+1)}{r^2}, \tag{3}$$

where μ is the reduced mass of the colliding pair [63–68]. The only unknown term is the nuclear potential term in the effective potential in Eq. (1). We use the microscopic Double Folding model potential for the real part of the nuclear potential in the optical model.

The real part of the nuclear potential was derived using a Double-Folding model with a realistic nucleon-nucleon interaction folded with the nuclear densities of projectile and target [69]. In the present case this describes the nuclear interaction between an alpha-particle and ^{12}C nucleus. The potential is given by the form

$$V_{DF}(\mathbf{R}) = N_R \int d\mathbf{r_1} \int \mathbf{dr_2}\rho_\alpha(\mathbf{r_1})\rho_{\mathbf{^{12}C}}(\mathbf{r_2})\mathbf{g}(\mathbf{E}, |\mathbf{s}|), \tag{4}$$

where ρ_α and $\rho_{^{12}C}$ are the density distributions of alpha-particle and ^{12}C and N_R is the normalization factor. $\mathbf{s}=\mathbf{R}+\mathbf{r}_2-r_1$ and $|\mathbf{s}|$ is the distance between a nucleon in the α-particle and a nucleon in the ^{12}C core. The density distribution form of the α-particle is a standard Gaussian coming from the scattering measurements

$$\rho_\alpha(\mathrm{r}_1) = 0.4299\exp(-0.7024\mathrm{r}_1^2).$$

The density distribution of the ^{12}C nucleus used in the present study has the form

$$\rho_{^{12}C}(\mathrm{r}_2) = \mathrm{C}\exp(-\alpha \mathrm{r}_2^2),$$

where C and α parameters can be deduced from the rms value of the radius ^{12}C that is 2.314 fm. In the present case we have used C=0.32 fm^{-3} and α=0.28 fm^{-2}. The M3Y nucleon-nucleon interaction, used in the double folding model, is given by two direct terms with different ranges, and by an exchange term with a delta interaction

$$\mathbf{g}(\mathbf{E}, |\mathbf{s}|) = 7999\frac{\exp(-4\mathrm{s})}{4\mathrm{s}} - 2134\frac{\exp(-2.5\mathrm{s})}{2.5} + \mathrm{J}_{00}\delta(\mathbf{s}).$$

The exchange term, J_{00}, is introduced to the M3Y interaction in order to guarantee the antisymmetrization of identical particles in the alpha cluster and in the ^{12}C core. Here it is given by the form $\mathrm{J}_{00}= -276(1 - 0.005\,\mathrm{E}_\alpha/\mathrm{m}_\alpha)$ [69, 70].

B. WKB Calculations

Since the ^{12}C nucleus does not have spherical shape, rather being oblate, deformation effects should also be included in the calculations. In the case of deformation, the effective potential between the α and ^{12}C nucleus can be constructed as

$$V_{eff}(r,\theta) = V_N(r,\theta) + V_L(r) + V_{\mathrm{C}}(r,\theta), \tag{5}$$

where θ is the deformation angle of the ^{12}C nucleus. Even if the Coulomb and centrifugal terms have the known forms in Eq.(5) there is a need to determine the shape of the nuclear potential [71, 72]. One notes that the form of the potential between α and core is very crucial to explain theoretical observables which are the excitation energies, electromagnetic transition rates, resonances [62] and the decay half lives of the nuclei [73, 74]. In the literature, different types potentials have been applied to obtain the interaction between the α and core. These include; the square well [2], Cosh potential [75], the optical potential derived from the experimental data [76], double folded potential based on M3Y [77, 78]. Recently, mean field type potentials have also been used to explain such systems [79], for example in the context of nuclear molecular structures [80]. In the present study, the Woods-Saxon-squared (WS2) potential for describing the α-^{12}C nuclear interaction is used with deformed a radius form is given by

$$V_{\mathrm{N}}(r,\theta) = -\lambda(\theta)\frac{V_0}{[1 + e^{\frac{r-R(\theta)}{a}}]^2}, \tag{6}$$

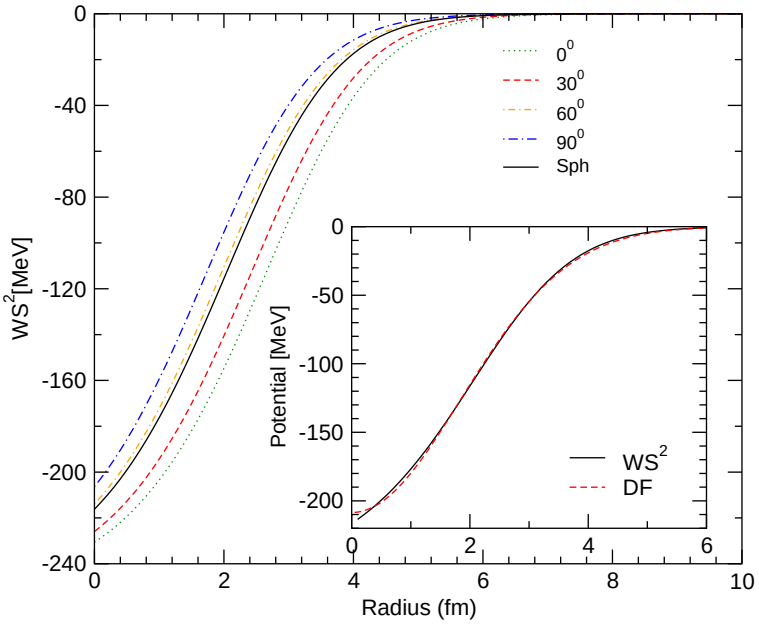

FIG. 1: The shape of Woods-Saxon-squared (WS2) potential versus radius at different angles. The resulting WS2 potential and the DF potential versus radius.

where V_0, $\lambda(\theta)$, R(θ) and a are the depth of the nuclear potential, the angle dependent normalization parameter, nuclear radius and diffuseness parameters, respectively. $\lambda(\theta)$ normalization paramater can be obtained with the Bohr-Sommerfeld quantization [41]. If one considers the quadrupole deformations, the nuclear radius in terms of the deformations is given by

$$R(\theta) = r_0 A_{\alpha}^{1/3} + r_0 A_{^{12}C}^{1/3}(1 + \beta_2 Y_{20}(\theta)), \tag{7}$$

where $A_{^{12}C}$, β_2 and Y_{lm} are the atomic mass number of the ^{12}C nucleus, quadrupole deformation parameter that is taken from Ref. [81] and the spherical harmonic, respectively.

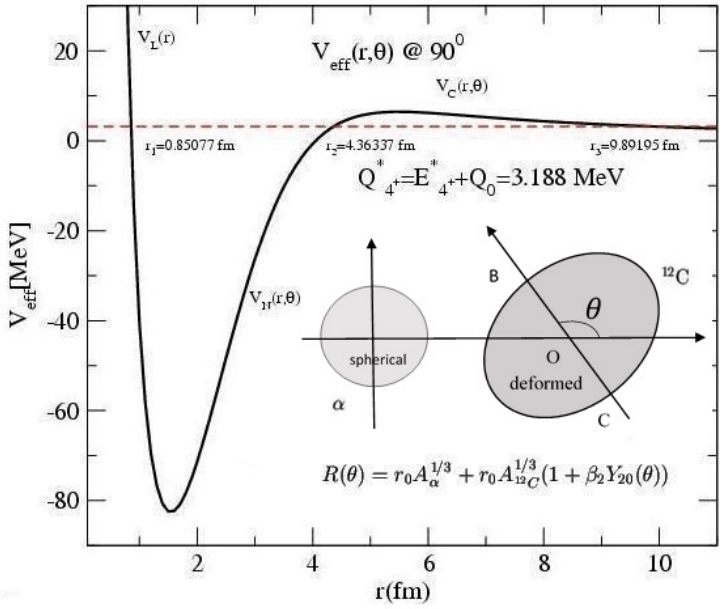

FIG. 2: The obtained turning points, Q value and $V_{eff}(r,\theta)$ at 90^0 together for 4^+ alpha decay of ^{16}O. Schematic illustration of the alpha and ^{12}C nucleus. It is noted that a cross section through an oblate nucleus looks prolate shape and COB is the axial symmetry axis of the ^{12}C.

The Langer modified centrifugal potential is used in the following form

$$V_L(r) = \frac{\hbar^2(L+\frac{1}{2})^2}{2\mu r^2}, \tag{8}$$

where L is the orbital angular momentum and μ is the reduced mass of the α and ^{12}C [82].

The Coulomb potential for deformation case in Eq. (2) is used with that R_C is taken as $R_C(\theta)$, in which $R_C(\theta) = R(\theta)$ is the Coulomb radius. Furthermore, the deformed form for Coulomb has a discontinuity at $r = R_C(\theta)$. To solve the problem, the following approximation is used [83],

$$\begin{aligned} \widetilde{V}_{\rm C}(r,\theta) &= \frac{Z_\alpha Z_{^{12}C} e^2}{r}(1 - e^{-\varphi(\theta)r - \frac{1}{2}(\varphi(\theta)r)^2 - 0.35(\varphi(\theta)r)^3}), \\ \varphi(\theta)R(\theta) &= \frac{3}{2}. \end{aligned} \tag{9}$$

There are three turning points for α decay energy: $r_1(\theta)$, $r_2(\theta)$ and $r_3(\theta)$, respectively. These can be calculated from the roots of $V_{eff}(r,\theta) = Q_\alpha$ depending on the deformation angle.

It should be noted that the alpha-decay energy from an excited state can be modified, e.g. by $Q_L^* = E_J^* + Q_0$, where Q_0 is the decay energy from the ^{12}C ground state, and E_J^* is the

excitation energy of a given state with the spin of J [80]. The turning points and $\lambda(\theta)$ are computed for each θ value in the the Bohr-Sommerfeld quantization as follows [25, 74, 84]:

$$\int_{r_1(\theta)}^{r_2(\theta)} dr\sqrt{\frac{2\mu}{\hbar^2}[Q_\alpha - V_{eff}(r,\theta)]} = (2n+1)\frac{\pi}{2} = (G-L+1)\frac{\pi}{2}, \tag{10}$$

where Q_α and n are the α-decay energy and the radial node quantum number explaining the interaction of the α-^{12}C, respectively. G is the global quantum number [85], coming from the Wildermuth rule given by

$$G = 2n + L = \sum_{i=1}^{4}(2n_i + \ell_i) = \sum_{i=1}^{4} g_i, \tag{11}$$

where g_i are the oscillator quantum numbers. In this prescription, G=8 and 9 are used for ^{16}O.

The alpha-decay width is given by [2, 25, 37, 84],

$$\Gamma_\alpha = PF\frac{\hbar^2}{4\mu}S, \tag{12}$$

where P is the preformation factor probability, F is the normalization factor and S is the transition probability of cluster nuclei, respectively. For simplicity, the preformation factor is used P =1.0 in the calculations [86]. The normalization factor F is obtained by [23, 24, 87]

$$F(\theta)\int_{r_1(\theta)}^{r_2(\theta)} dr\frac{1}{2k(r,\theta)} = 1, \tag{13}$$

where $k(r,\theta)$ is the wave number and it can be given by $k(r,\theta) = \sqrt{\frac{2\mu}{\hbar^2}(Q - V_{eff}(r,\theta))}$. The transition probabilities can be calculated from

$$S(\theta) = exp\Big[-2\int_{r_2(\theta)}^{r_3(\theta)} dr\kappa(r,\theta)\Big]. \tag{14}$$

$\bar{F}$ is the average value of the normalization factor integrated over the orientation angles and it can be calculated by using the following equation

$$\bar{F} = \frac{1}{\theta_{max} - \theta_{min}}\int_{\theta_{min}}^{\theta_{max}} d\theta F(\theta), \tag{15}$$

where θ_{max} and θ_{min} are maximum and minimum values of the orientation angles, and the average value of the transmission probability $\bar{S}$ are as follows [25, 41, 42]

$$\bar{S} = \frac{1}{\theta_{max} - \theta_{min}}\int_{\theta_{min}}^{\theta_{max}} d\theta S(\theta). \tag{16}$$

III. RESULTS

A. Optical Model Analysis; with no Deformation Dependence

The first set of baseline calculations that are presented in this section neglect any effects of deformation in ^{12}C. In these calculations, we use a nuclear potential that consists of a real DF potential and a Woods-Saxon-squared (WS2) for the imaginary potential

$$V_{Nuclear}(r) = V_{DF}(r) + i\frac{-W_0}{[1+e^{\frac{r-R_W}{a_W}}]^2}. \quad (17)$$

E_{lab}(MeV)	W_0(MeV)	r_{0W}(fm)	a_W(fm)	N_R
28.2	65.0	0.59	0.34	0.60
29.6	65.0	0.59	0.25	0.56
29.8	65.0	0.59	0.20	0.60
30.0	65.0	0.60	0.10	0.60
30.2	65.0	0.60	0.10	0.60
30.7	65.0	0.57	0.20	0.57
31.4	75.0	0.50	0.20	0.75
33.4	50.0	0.55	0.30	0.74
34.5	65.0	0.52	0.20	0.74
35.5	64.0	0.52	0.48	0.75

TABLE I: The parameters for WS2 imaginary potential and N_R used in the optic model calculations.

This has been used to fit elastic scattering data for the α+^{12}C reaction. In order to obtain the best agreement with the experimental data, we optimized the normalization factors in the Double Folding (DF) potential and the parameters in the WS2 imaginary potentials. The potential parameters used to fit the elastic scattering cross-sections for the α+^{12}C reaction over the energy range 28.2 to 35.5 MeV within the framework of the optical model formalism as shown in Table I, with fits in Fig. 3. The code DFPOT [88] was used for the microscopic DF potential calculation and the code FRESCO [89] was used to calculate the elastic scattering angular distributions. As can be seen in Fig. 3, there is a

reasonably good agreement between the elastic scattering experimental data and the results of the microscopic DF potential analysis for all energies. However, the microscopic potential

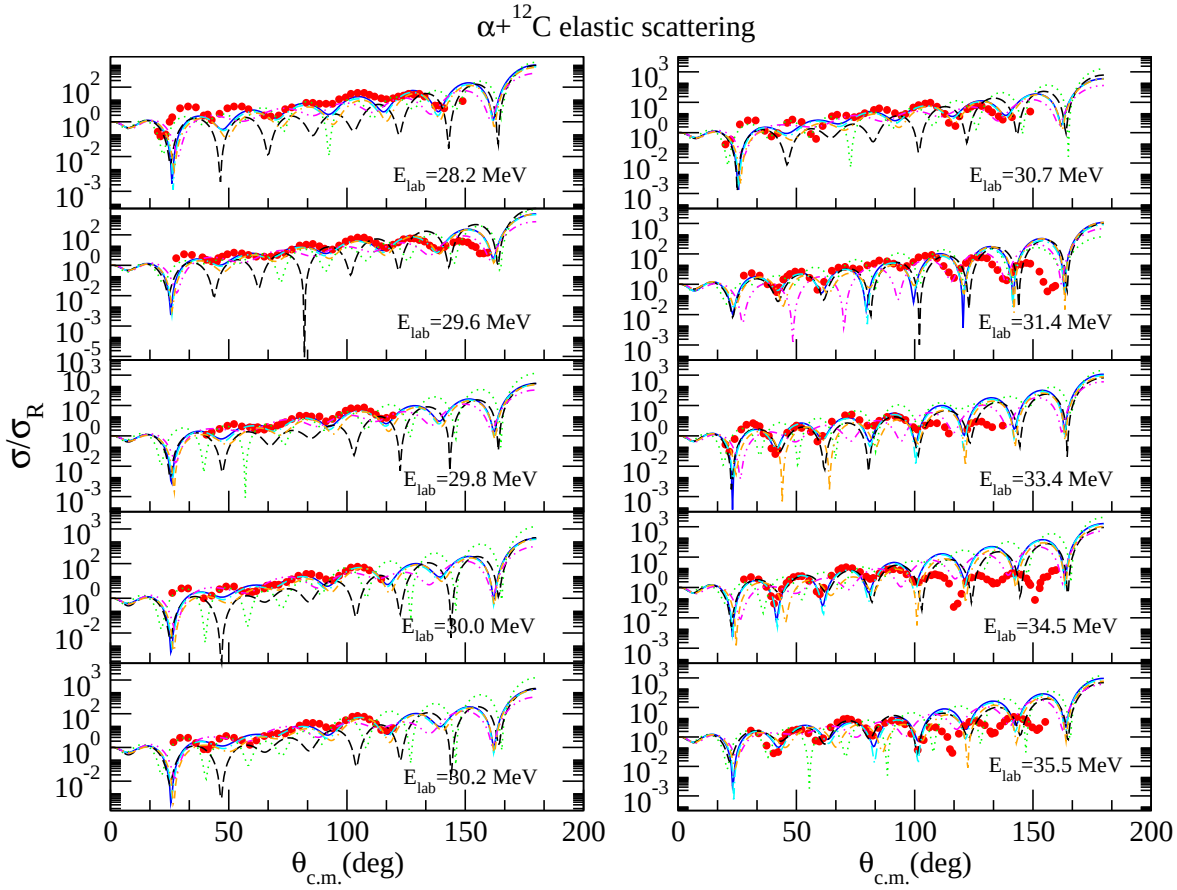

FIG. 3: The differential cross-sections of $\alpha + ^{12}C$ elastic scattering for E_{lab}=28.2 MeV- 35.5 MeV by analyzing DF potential and the deformed WS2 potential including the orientation angles. The experimental data are extracted from Ref.[58]. Here, red circle shows experimental data, solid line shows DF in blue, dotted line shows 0^o case in green, em-dashed line shows 30^o case in black, dot-em dash line shows 60^o case in cyan, dot-en-dot dash shows 90^o case in magenta, en-dot-en dash shows sph case in orange.

The present approach uses real part of the potential, which is DF potential, deduced from the elastic scattering data to consistently produce the characteristic of resonances in that same potential. Thus generating the resonance and elastic scattering spectrum on the same basis.

We used the same Double folding potential with $N_R = 1.00$ that reproduced the elastic

scattering data to obtain α-cluster states in ^{16}O by using Gamow code [62]. In these calculations, we have used G=8 and G=9 as global quantum numbers for positive and negative parity states, respectively. Given the nature of the potential, naturally this procedure does not exactly reproduce the experimental excitation energies. Hence, as a further step, we determined the values of the N_R normalization parameters that gave the known experimental excitation energy of 4^+ of ^{16}O state at E$_x$=10.356 MeV and 1^- of ^{16}O state at E$_x$=9.63 MeV. These were found to be $N_R = 0.9253$ and $N_R = 0.97871$ respectively. These values were then fixed in the calculations, separately, for positive and negative parity states. The Coulomb radius used here was $r_{0C} = 1.3$ fm. The results can be found in Table II. The excitation energies obtained with the Gamow code are in good agreement with experimental energies for positive parity states (average deviation 270 keV) but they are larger than the experimental values for negative parity states (average deviation 860 keV). In most part the widths predicted by the Gamow calculations, are in reasonable agreement with experiment, except at for the 5^- and 7^- states where the calculated excitation energies are at much higher energy than the experimental counterparts and hence the widths larger. It is notable that the Gamow code does not reproduce the width of the 4^+ state even though the energy of that state has been fixed. In order to better calculate the alpha decay widths using the WKB method the energies were fixed at the known experimental values, as shown in the last column of Table II. The width of the 4^+ state is much more closely reproduced by the WKB calculation. Overall the WKB method performed better with the average deviation from experiment is 280 keV compared with the 660 keV for the Gamow. Clearly, calculating the widths at the experimental energies is a large contributing factor.

B. WKB Calculations Including the Deformation of ^{12}C

This section describes a series of calculations in which the deformation of the ^{12}C nucleus is explicitly take into account. Here a Woods-Saxon-squared (WS2) potential form, Eq. (6), was used for the α-decay widths calculations in the WKB method. We have chosen to use a phenomenological Woods-Saxon-squared (WS2) potential since considering the deformations at different angles in microscopic DF potential is difficult. However, to maintain the consistency with the potential that was used in the elastic scattering data analysis, we have fitted the phenomenological WS2 potential to the DF potential and obtained the potential

St.	G	E_x [MeV]	Γ_α Exp [keV]	Ref.	E_x (Gamow) [MeV]	Γ_α (Gamow) [keV]	Γ_α(WKB) [keV]
0^+	8	6.05	–	[93]	5.03	–	–
2^+	8	6.92	–	[93]	6.54	0.05	–
4^+	8	10.35	27 ± 4	[93]	10.35	158	26.8
6^+	8	16.27	392 ± 20	[94]	16.24	367	448
8^+	8	–	–		25.33	641	–
1^-	9	9.63	400 ± 10	[93]	9.69	498	628
3^-	9	11.6	800 ± 100	[93]	11.89	898	– – –
5^-	9	14.66	632 ± 20	[94]	15.97	2220	1020
7^-	9	20.86	540 ± 100	[94]	24.04	2550	1270
9^-	9	–	–		33.26	3364	–

TABLE II: Excitation energy (Gamow code) and the decay widths (WKB) results with the DF model potential for ^{16}O, results have been fixed 4^+ and 1^- states for positive and negative parity states respectively. Here, $E_x = E + E_{threshold}$, $E_{threshold}$=7.162 MeV. The experimental values for 0^+, 2^+, 8^+ and 9^- states could not be obtained (−) and decay width for 3^- state was not calculated in WKB (− − −).

parameters: $V_0 = 253$ MeV, $a = 1.13$ fm and $r_0 = 0.73$ fm in Eq. (6). We have used $\beta_2 = 0.582$ for the deformation of ^{12}C [81]. The shape of Woods-Saxon-squared potential versus radius at different angles is seen in Fig. 1. The WS2 potential with the parameters that were obtained from fitting to the DF potential and the original DF potential, versus radius, are shown in the inset of Fig. 1.

By using the resulting deformed WS2 potential, we have calculated the α-decay widths in the framework of the WKB approach for (i) the spherical case, (ii) at different angles and (iii) averaged over all angles, Table III. The decay widths of the 4^+ state are different between the two set of the calculations in Table II it was 158 keV with Gamow code and in Table III closer to 30 keV with WKB method. It is noted that Gamow code is able to yield both the excitation energies and decay widths of resonant states, while the WKB method needs the decay energy as input and then gives the decay widths. Therefore the decay widths

calculated with the WKB method are in better agreement with the experimental data. The results presented here support the results of the study in Ref. [90].

In order to see the influence of deformations on the differential cross-sections of α+^{12}C elastic scattering, we have analyzed the differential cross-sections of α+^{12}C elastic scattering by using the deformed WS2 potential forms for different orientation angles. The deformed forms of WS2 potential for different angles for real part and same potential and parameters for imaginary part as the calculations in DF were directly used in the calculations. The obtained results are given together the results of DF potential in Fig. 3. It should be noted that as seen in this figure, the deformations with angles have also some influence on the differential cross-sections of α+^{12}C elastic scattering at different energies.

In order to illustrate the behavior of the turning points, we plot the turning points, Q value and $V_{eff}(r,\theta)$ at 90^0 for the 4^+ alpha decay of ^{16}O in Fig.2. It should be noted that when the angle increases from 0 to 90 degrees, the radius of potential decreases as seen in Fig. 1. For 90 degrees a more compact configuration is produced, similar to the tetrahedral structure found in the lowest energy configurations in the alpha cluster model. The 0 degree orientation, however, is associated with a more deformed, planar, alpha cluster model structure [91].

To understand the effect of the changing orientation, θ, we have examined $P = T^{cal}_{1/2}/T^{exp}_{1/2}$ [92]. In addition, we have also calculated the preformation factors $P_{sph} = \Gamma^{exp}_{\alpha}/\Gamma^{sph}_{\alpha}$ and $P_{all} = \Gamma^{exp}_{\alpha}/\Gamma^{all}_{\alpha}$, Table III. Here, Γ^{all}_{α} shows the calculated α-decay widths integrated over the all angles. Correspondingly, P_{sph} is the preformation factor for spherical case without deformation, whilst P_{all} represents the preformation factor for deformed system integrated over all angles. As seen in Table III, when the deformation of ^{12}C is taken into account in the calculations, the alpha decay widths change, clearly deformation plays a role. The variation of these WKB widths in terms of θ is shown in Fig. 4 for the 4^+ and 6^+ states. What is observed is that there is a systematic trend for the positive parity states (4^+ and 6^+) in which the width decreases towards $\theta = 90$ degrees. On the other hand, the proximity of the negative parity states to the top of the barrier leads to less robust results and in some cases no solution exists (as indicated by the $---$ in the table).

Importantly, the variation of angle, θ, corresponds to a change in the ^{12}C-α structure, with θ=0 corresponding to a planar structure and $\theta = 90$ a compact structure. From the behaviour of the 4^+ and 6^+ states, and a comparison with the experimental data (Fig. 4),

State	G	E_x[MeV]	Γ_α^{exp}[keV]	Γ_α^{sph}	Γ_α (0^o)	Γ_α (30^o)	Γ_α (60^o)	Γ_α (90^o)	Γ_α^{all}	$P_{sph.}$	P_{all}
4^+	8	10.35	27 ± 4	23.2	46.5	36.0	21.3	16.3	27.8	1.17	0.96
6^+	8	16.27	392 ± 20	362	826	623	322	226	452	0.34	0.87
1^-	9	9.63	400 ± 10	621	545	626	612	580	617	0.65	0.65
3^-	9	11.6	800 ± 100	749	$---$	$---$	795	906	963	1.07	0.83
5^-	9	14.66	632 ± 20	966	$---$	810	910	734	937	0.65	0.67
7^-	9	20.86	540 ± 100	1167	$---$	$---$	1059	749	1272	0.91	0.42

TABLE III: The α-decay widths (WKB) results in terms of keV with deformed Woods-Saxon squared (WS2) potential for different angles and over the all angles for ^{16}O. $---$ shows that the reasonable value could not obtained for the related states.

one would conclude that these states are more closely associated with the compact rather than planar structure.

C. Gamow Calculations

The conclusions reached in the WKB calculations can also be explored in the Gamow approach. Here we used potential sets that were obtained from WKB analysis in Section III B, but as before, to constrain the potential, the calculations were fixed by the excitation energy of 4^+ state and 1^- for positive and negative parity states, respectively. As described earlier this requires the potential to be re-normalized (E_x=10.35 and E_x=9.63 MeV). Here we have used the $\lambda(\theta)$ values (in Eq. 6) determined for each cases: $\lambda(\theta) = 0.886, 0.9297$ for sph. case, $\lambda(\theta) = 0.601, 0.6332$ for 0^0, $\lambda(\theta) = 0.690, 0.7197$ is for 30^0, $\lambda(\theta) = 0.934, 0.9765$ is for 60^0, $\lambda(\theta) = 1.107, 1.1376$ is for 90^0. We have then calculated resonant state energies using the Gamow code with the WS2 potential at different angles for ^{16}O as can be seen in Table IV.

We have plotted the corresponding excitation energies of ^{16}O versus $J(J+1)$ for G=8, positive parity states, and G=9, negative parity states, as seen in Fig. 5 and Fig. 6, respectively. Moreover, by calculating the average rotational slope, we have obtained the corresponding values of the rotational gradient, $\hbar^2/2I$. As seen from both figures the values for $\hbar^2/2I$, the gradient increases when the angle is changed from 0 to 90 degrees and the

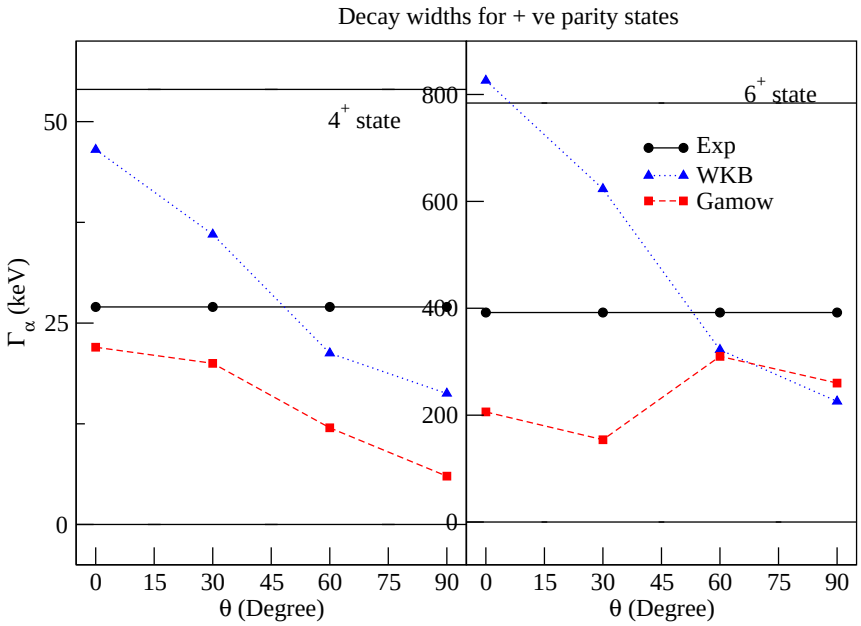

FIG. 4: The calculated alpha decay widths with Gamow and WKB in terms of keV versus angles. Here the straight line shows the experimental values with error bars, the dashed line shows Gamow results, the dotted line shows WKB results for positive parity states. All results were fixed by the excitation energy of 4^+ state.

biggest values are at 90 degree both for positive and and negative parity states. Since a large gradient means a small moment of inertia, this would correspond to a more compact structure for ^{16}O. Consequently, this result is consistent with the expectation that $\theta = 90$ degrees should be the most compact configuration.

In addition, as observed in the calculations for the 4^+ state (Fig. 4), the width is also sensitive to the potential shape, with a reduction in width for the more compact case; 90 degrees. This is consistent with the WKB calculations, though for the Gamow calculations the width is consistently under predicted. The systematic reduction in the width with angle is not seen for the Gamow calculations of the 6^+ state as its excitation energy is not fixed and varies with θ. Since different centrifugal and Coulomb potentials are used for the Gamow and WKB calculations this clearly causes some difference in the results. Even though the Gamow results for decay widths are better in principle, when widths are small computational difficulties arise and in such cases the WKB method is preferable.

				$E_x[MeV], \Gamma_\alpha[keV]$(Gamow code)				
St.	G	E_x[MeV]	Γ_α^{exp}[keV]	sph.	0^o	30^o	60^o	90^o
0^+	8	6.05	–	5.31	6.89	6.37	5.06	4.23
2^+	8	6.92	–	6.90	7.94, 8	7.60	6.72	6.17
4^+	8	10.35	27 ± 4	10.35, 18	10.37, 22	10.33, 20	10.34, 12	10.34, 6
6^+	8	16.27	392 ± 20	15.86, 242	14.20, 206	14.79, 154	16.13, 310	16.95, 260
8^+	8	–	–	24.08, 348	19.64, 106	21.15, 222	24.72, 492	26.78, 512
1^-	9	9.63	400 ± 10	9.63, 326	9.63, 236	9.63, 309	9.63, 186	9.63, 107
3^-	9	11.6	800 ± 100	12.62, 662	11.49, 1055	12.58, 938	12.63, 646	12.72, 694
5^-	9	14.66	632 ± 20	16.62, 1421	15.03, 933	16.88, 2094	16.66, 1225	16.96, 1097
7^-	9	20.86	540 ± 100	24.94, 2514	21.32, 2042	22.16, 1538	25.06, 2252	25.76, 2052
9^-	9	–	–	35.81, 2882	27.86, 1569	31.08, 2018	36.20, 2416	41.63, 1958

TABLE IV: Resonant State energies (Gamow) in terms of MeV and alpha decay widths in terms of keV with WS2 potential for ^{16}O. Here $E_x = E + E_{threshold}$, $E_{threshold} = 7.162MeV$. While – shows that the experimental values do not exist for these states, results were fixed by the excitation energy of 4^+ state and 1^- for positive and negative parity states, respectively.

D. Branching Ratios

Finally, in order to use the experimentally measured branching ratios of decay of ^{16}O [48], we have calculated alpha decay widths for the decay to the 2^+ excited state of ^{12}C for spherical case and different angles in the WKB method as seen in Table V. When combined with the decay to the ground state of ^{12}C (Table III) this would give the total width for each state. Here, the excitation energy of the 2^+ state is 4.438 MeV which is added to Q-value for g.s is 7.1619 MeV in the calculation of the threshold for the decay process. As before the proximity of the 7^- state to the barrier resulted in non convergence for the calculations. For other states marked with a "–" the decay was below threshold for the ^{12}C(2^+) decay; 11.6 MeV. The calculations for the branching ratios indicate that there is not a strong sensitivity to the angle, θ, in that the ratio between ground state and excited state does not vary significantly.

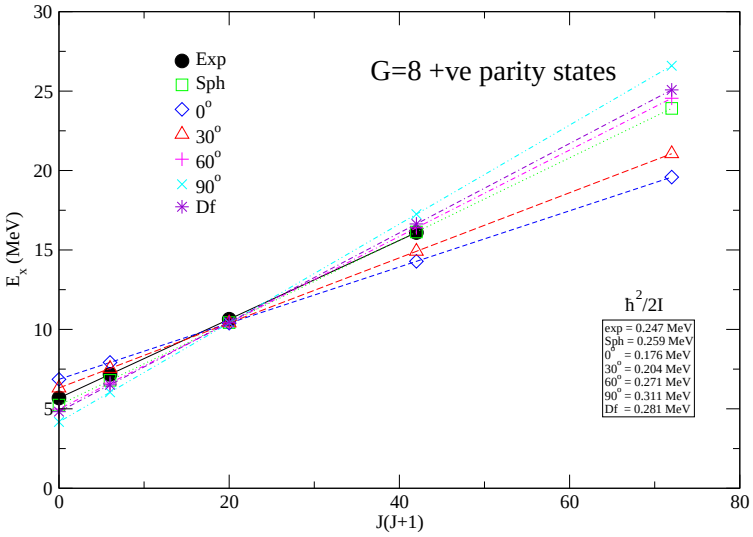

FIG. 5: Excitation energy spectrum of ^{16}O versus J(J+1) for G=8, + ve parity states. All results were fixed by the excitation energy of 4^+ state.

However, in Ref. [48], high resolution measurements of absolute alpha decay widths in ^{16}O have been performed and they extracted information about branching ratios of different decay modes. These experiments indicate a strong preference for the decay to the ^{12}C ground state with close to 100% branching ratios. The present calculations indicate that there should be a significant component for the 5^- and 6^+ states to decay to the ^{12}C(2^+) state. Given that this is not observed experimentally, it indicates that the underlying structure of the states in ^{16}O resembles $^{12}C_{gs}+\alpha$ in which the spin of the ^{16}O nucleus arises from the orbital motion of the α-particle around the ^{12}C "core".

IV. DISCUSSION AND CONCLUSIONS

The calculations presented explore the effect of the angular orientation of the ^{12}C nucleus with respect to the axis connecting the α-particle on the properties of the states of ^{16}O. The aim was to determine if this approach reveals useful structural information which may, for example, be linked to Alpha Cluster Model (ACM) calculations such as those in Ref. [91]. In these ACM calculations, the set of states associated with the experimental band heads at 6.05

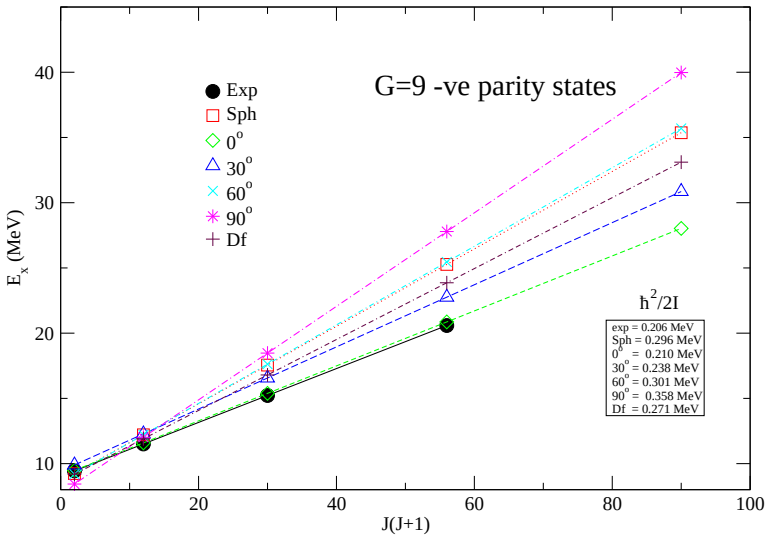

FIG. 6: Excitation energy spectrum of ^{16}O versus J(J+1) for G=9, - ve parity states. All results were fixed by the excitation energy of 1^- state.

			Γ^{exp} [48]			Γ_α^{calc} (keV)									
			Γ_{tot}	$\Gamma_\alpha/\Gamma_{tot}$		Sph.		0^o		30^o		60^o		90^o	
State	G	E_x		^{12}C(g.s.)	^{12}C*(2^+)	g.s.	2^+	g.s.	2^+	g.s.	2^+	g.s.	2^+	g.s.	2^+
0^+	8	6.05	Bound	–	–	–	–	–	–	–	–	–	–	–	–
2^+	8	6.92	Bound	–	–	–	–	–	–	–	–	–	–	–	–
4^+	8	10.35	26(3)	0.86(9)	–	23.2	–	46.5	–	36	–	21.3	–	16.3	–
6^+	8	16.27	420(20)	0.982(48)	–	362	302	826	525	623	432	322	281	226	223
1^-	9	9.63	420(20)	~ 1	–	620	–	545	–	626	–	612	–	580	–
3^-	9	11.60	800(100)	1	–	749	–	–	–	–	–	795	–	906	–
5^-	9	14.66	670(15)	1.002(42)	–	966	298	–	298	810	252	910	176	734	147
7^-	9	20.86	900(60)	1.16(23)	–	1167	–	–	–	–	–	1059	1758	1272	1657

TABLE V: Comparison the experimental decay widths in Ref.[48] and the calculated ones with WKB for ^{12}C(g.s.) and ^{12}C*(2^+) decay modes of ^{16}O.

MeV (0^+) and 9.63 MeV (1^-) produce positive and negative parity rotational bands. These states are those shown in Table II and have been linked to planar-like structures in which the oblate ^{12}C nucleus is orientated such that the angle of rotation would be equivalent to 0° in the present calculations. An angle of 90° corresponds to more compact structure closer to a

tetrahedral arrangement of the α-particles. In the ACM this would be a structure which has been linked to the ^{16}O ground-state. However, the Algebraic Cluster Model [95] approach appears to indicate that these excited states might also have a tetrahedral structure. There is a clear contradiction between the Alpha and Algebraic Cluster Models.

In the present calculations the approach has been to constrain the nature of the interaction potential through the reproduction of elastic scattering data and then through the WKB and Gamow methods understand if the calculated excitation energies and widths reveal a structural signature. In this instance, the widths are sensitive to the nature of the barrier which has an angular dependence and the systematics of the excitation energies follow a rotational-like behavior linked to the radial extent of the potential, which also has an angular dependence.

In interpreting the present approach, the first thing to note is that the negative parity states reside very close to the top of the barrier and hence the sensitivity of the widths to the changes in the barrier with orientation of the ^{12}C is minimal and hence no reliable information may be extracted. For example, for the 9.63 MeV, 1^-, the experimental width is 400(10) keV as shown in Table III. This is broadly reproduced by all of the calculations independent of angle. Clearly, the experimental width is dominated by the proximity to the top of the barrier, rather than the details of the barrier.

On the other hand, the positive parity states, in some cases, show a sensitivity to the barrier in both the WKB calculations, Table III, and Gamow calculations, Table IV. The Gamow calculations show an angular dependence for the width of the 4^+ state, but not 6^+. This latter observation is due to the energy of the 4^+ state being fixed in the Gamow calculations and the model being used to predict the energy of the other states. It is concluded that since in the WKB approach the energy is fixed at the experimental energy a more reliable result is expected. Indeed the widths as a function of angle for both the 4^+ and 6^+ states span the experimental value. The analysis would indicate that of the two limiting orientations, the 90° is preferred over the 0° possibility for the positive parity band.

Figures 5 and 6 showed the experimental energy-spin systematics for the two bands compared with the systematics for the Gamow calculations for different angular orientations of the ^{12}C nucleus. In the case of the positive parity states, there is closer agreement with larger angle orientations (θ=90 degrees), also consistent with the WKB conclusions. It is seen for the negative parity states that the experimental sequence lies closer to the 0° possibility.

However, as noted before, due to the proximity of the states to the top of the barrier, the validity of the calculations for these states is questionable. The conclusion would appear to be from the analysis of the positive parity states that more compact configurations, i.e. tetrahedral, rather than planar, are favored.

The branching ratio for the decay of the ^{16}O states to the ground and first excited state of ^{12}C was calculated and although showed little sensitivity to the ^{12}C orientation, did reveal that the experimental decay to the $^{12}C_{gs}$ channel is enhanced compared with calculation indicating that the structure of ^{16}O may be described in terms of an α-particle orbiting a ^{12}C core.

The calculations demonstrate that deformation, and orientation, effects are extremely important in determining the properties of the excited states in ^{16}O and in principle the technique developed here could be applied to other systems to develop a more systematic understanding of how spectroscopic properties such as decay widths may be linked to the underlying nuclear structure. This includes the important question as to how to decouple the cluster preformation probability from the variation of the decay barrier with the deformed core+α orientation.

Acknowledgments

This work was supported by the Turkish Science and Research Council (TÜBİTAK) with Grant Number 113F225.

[1] A. Arima, H. Horiuchi, K. Kubodera, and N. Takigawa, Clustering in Light Nuclei, Advances in Nuclear Physics, edited by M. Baranger and E. Vogt, Vol. 5 (Plenum, New York, 1973), p. 345.

[2] B. Buck, A. C. Merchant and S. M. Perez, J. Phys. G: Nucl. Part. Phys. **17**, 1223 (1991).

[3] R. K. Sheline and K. Wildermuth, Nucl. Phys. **21**, 196 (1960).

[4] B. Buck, C. B. Dover and J. P. Vary, Phys. Rev. C **11**, (5), 1803 (1975).

[5] M. Freer and A. C. Merchant, J. Phys. G: Nucl. Part. Phys. **23**, 261 (1997).

[6] H. Horiuchi and K. Ikeda, Cluster Model of the Nucleus, International Review of Nuclear Physics, edited by T. T. S. Kuo and E. Osnes (World Scientific, Singapore, 1985), Vol. 4, pp. 1258.

[7] H. J. Rose and G. A. Jones, Nature (London) **307**, 245 (1985).

[8] F. Michel, et al., Phys. Rev. C **28**, 1904 (1983).

[9] B. Buck, et al., Phys. Rev. C **52**, 1840 (1995).

[10] F. Michel, G. Reidemeister, S. Ohkubo, Phys. Rev. Lett. **57**, 1215(1986).

[11] F. Michel, et al., Prog. Theor. Phys. Suppl. **132**, 7 (1998).

[12] J. Wauters *et al.,* Phys. Rev. Lett. **72**, 1329 (1994).

[13] S. Hofmann *et al.,* Eur. Phys. J. A **10**, 5 (2001).

[14] Yu. Ts. Oganessian *et al.,* Phys. Rev. C **74**, 044602 (2006); **70**, 064609 (2004).

[15] M. Freer *et al.,* Phys. Rev. Lett. **96**, 042501 (2006).

[16] K. P. Santhosh, and B. Priyanka, Journal of Physics G: Nuclear and Particle Physics **39**, 085106 (2012).

[17] F. R. Xu *et al.,* Journal of Physics: Conference Series. Vol. 436. No. 1., (2013).

[18] D. D. Poenaru, R. A. Gherghescu, and W. Greiner, Rom. Journal of Physics **58**, 1157 (2013).

[19] K.P. Santhosh, B. Priyanka, and M. S. Unnikrishnan, Int. Conf. on Recent Trends in Nuclear Physics-2012: ICRTNP-2012. Vol. 1524. No. 1., (2013).

[20] M. Ismail, A. Adel, Phys. Rev. C **89**, 034617 (2014).

[21] V. Yu. Denisov, Phys. Rev. C **88**, 044608 (2013).

[22] G. Gamow, Z. Phys. **51**, 204 (1928).

[23] S.A. Gurvitz, G. Kalbermann, Phys. Rev. Lett. **59**, 262. B (1987).

[24] B. Buck, J.C. Johnston, A.C. Merchant, S.M. Perez, Phys. Rev. C **53** 2841 (1996).

[25] F. Koyuncu, A. Soylu, and O. Bayrak, Modern Physics Letters A **32**, 1750050 (2017).

[26] D. S. Delion, A. Sandulescu, and W. Greiner, Phys. Rev. C **69**, 044318 (2004).

[27] D. S. Delion, R. J. Liotta, and R. Wyss, Phys. Rev. C **76**, 044301 (2007).

[28] C. Xu and Z. Ren, Phys. Rev. C **75**, 044301 (2007).

[29] C. Xu, Z. Ren, and Y. Guo, Phys. Rev. C **78**, 044329 (2008).

[30] J. C. Pei, F. R. Xu, Z. J. Lin, and E. G. Zhao, Phys. Rev. C **76**, 044326 (2007).

[31] G. L. Zhang, X. Y. Le, and H. Q. Zhang, Phys. Rev. C **80**, 064325 (2009).

[32] D. Ni and Z. Ren, Phys. Rev. C **81**, 024315 (2010).
D. Ni and Z. Ren, Phys. Rev. C **81**, 064318 (2010).

[33] D. Ni and Z. Ren, Phys. Rev. C **84**, 037301 (2011).

[34] D. Ni and Z. Ren, Phys. Rev. C **83**, 067302 (2011).

[35] Y. Qian, Z. Ren, and D. Ni, Phys. Rev. C **83**, 044317 (2011).

[36] Y. Qian and Z. Ren, Phys. Rev. C **84**, 064307 (2011).

[37] V. Yu. Denisov and A. A. Khudenko, At. Data Nucl. Data Tables **95**, 815 (2009).

[38] V. Yu. Denisov and A. A. Khudenko, Phys. Rev. C **80**, 034603 (2009).

[39] V. Yu. Denisov and A. A. Khudenko, Phys. Rev. C **81**, 034613 (2010).

[40] M. Ismail,W. M. Seif, A Y Ellithi and F Salah, J. Phys. G: Nucl. Part. Phys. **35**, 075101 (2008).

[41] A. Coban, O. Bayrak, A. Soylu, I. Boztosun, Phys. Rev. C **85**, 044324 (2012).

[42] A. Soylu, Y. Sert, O. Bayrak, and I. Boztosun, Eur. Phys. J. A **48** 128 (2012).

[43] P. Chevallier, *et al.*, Physical Review **160**, 827 (1967).

[44] F. Brochard, P. Chevallier, D. Disdier, V. Rauch , G. Rudolf, and F. Scheibling , Physical Review C **13**, 967-975 (1976).

[45] L. L. Ames, Ph.D. thesis, University of Wisconsin, Madison, 1979.

[46] M. Freer, *et al.* Phys. Rev. C **51**, 1682 (1995).

[47] M. Freer, *et al.* Phys. Rev. C **70**, 064311 (2004).

[48] C. Wheldon, *et al.* Phys. Rev. C **83**, 064324 (2011).

[49] Y. Funaki, T. Yamada, A. Tohsaki, H. Horiuchi, G. Röpke, and P. Schuck, Phys. Rev. C **82**, 024312 (2010).

[50] K. C. W. Li, et al, Phys. Rev. C **95**, 031302 (2017).

[51] M. Freer, Journal of Physics: Conference Series. Vol. 590. No. 1. IOP Publishing, (2015).

[52] N. Curtis, et al. Phys. Rev. C **94** 034313 (2016).

[53] B. Buck, C. B. Dover and J. P. Vary, Phys. Rev. C **11** 1803 (1975).

[54] B. Buck and J. A. Rubio, J. Phys. G: Nucl. Phys. **10** 209-211 (1984).

[55] R. A. Baldock, B. Buck and J. A. Rubio, Nuclear Physics A **426** 222-252 (1984).

[56] R. A. Baldock and R. A. Stratton, J. Phys. G: Nucl. Phys. **11** 515-525 (1985).

[57] M. Katsuma, J. Phys. G **40**, 025107 (2013).

[58] M. Katsuma, EPJ Web of Conferences **66**, 03 0 41 (2014).

[59] S. Ohkubo, Y. Hirabayashi, Physics Letters B **684** 127131 (2010).

[60] C. j. Halcrow, C. King, and N. S. Manton, Phys. Rev. C **95**, 031303 (2017).

[61] R. Bijker,F. Iachello, Nuclear Physics A **957**, 154-176 (2017).

[62] T. Vertse, K. F. Pal and Z. Balogh, Comp. Phys. Comm. **27**, 309 (1982).

[63] G. R. Satchler, Nucl. Phys. A **409**, 3c (1983).

[64] I. Boztosun and W. D. M. Rae, Phys. Lett. B **518** 229 (2001).

[65] I. Boztosun, O. Bayrak, and Y. Dagdemir, Int. J. Mod. Phys. E **14**, 663 (2005).

[66] I. Boztosun and W. D. M. Rae, Phys. Rev. C **63**, 054607 (2001).

[67] G. Kocak, M. Karakoc, I. Boztosun, and A. B. Balantekin, Phys. Rev. C **81**, 024615 (2010).

[68] I. Boztosun, Phys. Rev. C **66**, 024610 (2002).

[69] G. R. Satchler and W.G. Love, Physics Reports (Review Section of Physics Letters) **55**, No.3 (1979) 183-254.

[70] M. Karakoc and I. Boztosun, Phys. Rev. C **73**, 047601 (2006).

[71] G. Igo, Phys. Rev. Lett. **1**, 72 (1958).
G. Igo, Phys. Rev. **115**, 1665 (1959).

[72] J. Cook, J. M. Barnwell, N. M. Clarke and R. J. Griffiths, J. Phys. G: Nucl. Phys. **6**, 1251 (1980).

[73] B. Buck, J. C. Johnston, A. C. Merchant and S. M. Perez, Phys. Rev. C **52**, 1840 (1995).

[74] B. Buck, A. C. Merchant and S. M. Perez, Phys. Rev. Lett. **72**, 1326 (1994).
B.Buck A. C. Merchant and S. M. Perez, Phys. Rev. Lett., **76**, 380, (1996).

[75] Buck et al., Phys. Rev. Lett. **65**, 2975 (1990);

[76] C. Xu and Z. Ren, Phys. Rev. C **69**, 024614 (2004).

[77] Z. Z. Ren, C. Xu, and Z. Wang, Phys. Rev. C **70**, 034304 (2004).

[78] C. Xu and Z. Ren, Nucl. Phys. A **753**, 174 (2005); A760, 303 (2005).

[79] F. R. Xu and J. C. Pei, Phys. Lett. B **642**, 322 (2006).

[80] J. C. Pei and F. R. Xu, Phys. Lett. B **650**, 224 (2007).

[81] T. Belgya, O. Bersillon, R. Capote, T. Fukahori, G. Zhigang, S. Goriely, M. Herman, A.V. Ignatyuk, S. Kailas, A. Koning, P. Oblozinsky, V. Plujko and P. Young. Handbook for calculations of nuclear reaction data, RIPL-2. IAEA-TECDOC-1506 (IAEA, Vienna, 2006). Available online at http://www-nds.iaea.org/RIPL-2/.

[82] R. E. Langer , Phys. Rev., **51**, 669, (1937).

[83] D. M. Brink and N. Takigawa, Nucl. Phys. A **279**, 159 (1977).

[84] C. Xu and Z. Ren, Phys. Rev. C **74**, 014304 (2006).

[85] K. Wildermuth and Y. C. Tang, "A Unified Theory of the Nucleus", New York, (1997).

[86] P. E. Hodgson, E. Běták, Physics Reports **374**, 1 (2003).

[87] C. Xu, Z. Ren, Phys. Rev. C **68** (2003) 034319.

[88] J. Cook, Comput. Phys. Commun. **25**, 125 (1982).

[89] I. J. Thompson, Comput. Phys. Rep. **7**, 167 (1988).

[90] S. Mahadevan, P. Prema, C. S. Shastry, and Y. K. Gambhir, Phys. Rev. C **74**, 057601 (2006).

[91] W. Bauhoff, H. Schultheis, and R. Schultheis, Physical Review C **29**, 1046 (1984).

[92] T. T. Ibrahim and S. M. Wyngaardt, J. Phys. G: Nucl. Part. Phys. **41**, 055111 (2014).

[93] F. Ajzenberg-Selove Nucl. Phys. A **375**, 1 (1982).

[94] L. L. Ames Phys. Rev. C **25**, 729 (1982).

[95] R. Bijker and F. Iachello, Phys. Rev. Lett. **112**, 152501 (2014).